Redox-Dependent Acetyl Transfer Partial Reaction of the Acetyl-CoA Decarbonylase/Synthase Complex: Kinetics and Mechanism†

B. Bhaskar,‡ Edward DeMoll,*,§ and David A. Grahame*,‡

Department of Biochemistry and Molecular Biology, Uniformed Services University of the Health Sciences, Bethesda, Maryland 20814-4799, and Department of Microbiology & Immunology, Chandler Medical Center, University of Kentucky, Lexington, Kentucky 40536-0084

Received May 26, 1998; Revised Manuscript Received July 29, 1998

ABSTRACT: Acetyl-CoA decarbonylase/synthase (ACDS) is a multienzyme complex that plays a central role in energy metabolism in *Methanosarcina barkeri* grown on acetate. The ACDS complex carries out an unusual reaction involving net cleavage of the acetyl C−C and thioester bonds of acetyl-CoA. The overall reaction is composed of several partial reactions, one of which involves catalysis of acetyl group transfer. To gain insight into the overall reaction, a study was carried out on the kinetics and mechanism of the acetyltransferase partial reaction. Analysis by HPLC was used to quantify rates of acetyl transfer from acetyl-CoA both to 3′-dephospho-CoA and, by isotope exchange, to ^{14}C-labeled CoA. Acetyl transfer activity was observed only under strongly reducing conditions, and was half-maximal at −486 mV at pH 6.5. The midpoint activation potential became increasingly more negative as the pH was increased, indicating the involvement of a protonation step. Cooperative dependence on acetyl-CoA concentration was exhibited in reactions that contained incompletely reduced enzyme; however, under redox conditions supporting maximum activity, hyperbolic kinetics were found. A ping-pong steady state kinetic mechanism was established, consistent with formation of an acetyl-enzyme intermediate. Analysis of the inhibitory effects of CoA on acetyl transfer to 3′-dephospho-CoA provided values for K_i^{CoA} of 6.8 μM and for $K_i^{acetyl-CoA}$ of 45 μM; isotope exchange analyses yielded values of 32 and 120 μM, respectively. Two separate measures of stability yielded values for the free energy of hydrolysis of the acetyl-enzyme intermediate of −9.6 and −9.3 kcal/mol, an indication of a high-energy bonding interaction in the acetyl-enzyme species. Implications for the mechanism of C−C bond cleavage are discussed.

Fragmentation of the acetyl C−C bond occurs as an early step in the pathway of acetate conversion to carbon dioxide and methane in *Methanosarcinae*. This cleavage is brought about by a multienzyme complex that catalyzes the decarbonylation of acetyl-CoA. The enzyme complex, which we designate acetyl-CoA decarbonylase/synthase (ACDS[1]), is composed of five different subunits (α, β, γ, δ, and ϵ), and carries out the reversible cleavage of acetyl-CoA, as described by eq 1:

$$\text{acetyl-CoA} + H_4\text{SPt} + H_2O \rightleftharpoons CH_3\text{-}H_4\text{SPt} + CO_2 + \text{CoASH} + 2H^+ + 2e^- \quad (1)$$

in which H_4SPt and CH_3-H_4SPt stand for methanogen H_4 folate analogues tetrahydrosarcinapterin and N^5-methyltetrahydrosarcinapterin, respectively. Reaction 1 is made up of several partial reactions, involving (a) acetyl transfer from acetyl-CoA to the enzyme, (b) decarbonylative cleavage of the enzyme-acetyl C−C bond, (c) oxidation of the carbonyl fragment to CO_2, and (d and e) stepwise transfer of the methyl moiety to an enzyme-bound B_{12} cofactor and then to H_4SPt. For three of these activities, specific subunits and/or subcomponent proteins of the ACDS complex have been identified. It has been known for some time that a protein component composed of the α and ϵ subunits carries out oxidation of CO (reaction 2), suggesting participation in oxidation of the carbonyl fragment.

$$CO + H_2O \rightleftharpoons CO_2 + 2H^+ + 2e^- \quad (2)$$

A second protein component $\gamma\delta$, which contains a bound corrinoid cofactor, catalyzes reversible methyl group transfer to H_4SPt according to eq 3 (*1*).

$$CH_3\text{-cob(III)amide}-\text{protein} + H_4\text{SPt} \rightleftharpoons \text{cob(I)amide}-\text{protein} + CH_3\text{-}H_4\text{SPt} + H^+ \quad (3)$$

The third isolated activity, that of acetyl group transfer (reaction 4), was found to reside on the β subunit (*1*).

$$E_\beta + \text{acetyl-CoA} \rightleftharpoons E_\beta\text{-acetyl} + \text{CoA} \quad (4)$$

† This work was supported by grants from the National Science Foundation (MCB-9630488) and the U.S. Department of Energy (DE-FG02-97ER20270).

* To whom correspondence should be addressed.

‡ Uniformed Services University of the Health Sciences.

§ University of Kentucky.

[1] Abbreviations: ACDS, acetyl-CoA decarbonylase/synthase; CH_3-H_4SPt, N^5-methyltetrahydrosarcinapterin; H_4SPt, tetrahydrosarcinapterin; Fd, ferredoxin; CODH/ACS, carbon monoxide dehydrogenase/acetyl-CoA synthase; HPLC, high-pressure liquid chromatography; MOPS, 3-(*N*-morpholino)propanesulfonic acid; E_o, standard reduction potential; NHE, normal hydrogen electrode.

S0006-2960(98)01242-2 CCC: $15.00
Published on Web 09/23/1998

A convenient, nonradioactive assay for acetyl transfer activity was developed on the basis of quantitative HPLC measurements using 3′-dephospho-CoA, an acetyl acceptor substrate chromatographically distinguishable from CoA, according to reaction 5.

$$\text{acetyl-CoA} + \text{3′-dephospho-CoA} \rightleftharpoons \text{CoA} + \textit{S}\text{-acetyl-3′-dephospho-CoA}\ K_{eq} = 1.00 \pm 0.05^{2} \quad (5)$$

The acetyltransferase reaction (eq 5) is analogous to the acetyl-CoA/CoA isotope exchange reaction (eq 6), originally detected by Pezacka and Wood (*2*), and later studied by others (*3*, *4*) in preparations containing *Clostridium thermoaceticum* CO dehydrogenase/acetyl-CoA synthase (CODH/ACS), and also examined in the *Methanosarcina thermophila* ACDS complex (*5*).

$$\text{acetyl-CoA} + \text{CoA*} \rightleftharpoons \text{CoA} + \text{acetyl-CoA*} \quad (6)$$

Studies carried out on clostridial CODH/ACS by Lu and Ragsdale (*4*) demonstrated that CoA exchange activity is strongly dependent on low redox potential. Various authors have interpreted the ability to catalyze acetyl transfer as evidence for the formation of an acetyl-enzyme intermediate. This intermediate is suspected to be the species that undergoes direct scission of the C−C bond. Knowledge of the reactivity of this intermediate is therefore essential to understanding the mechanism of C−C bond cleavage. Ultimately, this requires characterization of the physicochemical properties of the acetyl-enzyme intermediate. However, as yet, the enzyme-acetyl intermediate has not been observed spectroscopically or physically isolated, and much remains to be learned about its properties.

The existence of an acetyl-enzyme intermediate would lead to a prediction of a ping-pong kinetic pattern for both reactions 5 and 6. However, until now, the kinetic mechanisms of these reactions were unknown, presenting a complication for interpretation of kinetic parameters. Kinetic analysis of A ⇌ P exchange processes are capable of providing information about the thermodynamic stability of the enzyme intermediate F in a ping-pong mechanism based on the K_i^P/K_i^A ratio (*6*). This provided a means of obtaining information about the characteristics of the acetyl-enzyme intermediate (intermediate F) relevant to its inherent ability to undergo C−C bond cleavage. Herein, studies on the CoA exchange and acetyltransferase reactions 5 and 6 now establish a ping-pong kinetic mechanism. Values were determined for true kinetic parameters K_m and k_{cat}, and for additional parameters directly reflecting binding of substrates $K_i^{acetyl-CoA}$ and K_i^{CoA}. Studies on the pH and redox dependence indicate that the reductive activation process contains a step involving proton transfer. Thermodynamic information obtained on acetyl transfer reaction 4 indicates a high-energy bonding interaction in the acetyl-enzyme intermediate. This work constitutes the first comprehensive kinetic study of ACDS acetyl transfer reactivity, and the first measurement of a characteristic thermodynamic property of the acetyl-enzyme intermediate.

[2] D. A. Grahame and E. DeMoll, unpublished results.

MATERIALS AND METHODS

Reagents. Coenzyme A, disodium salt (>96%, HPLC), acetyl-CoA, trilithium salt (>95%, HPLC), and vitamin B_{12a} (aquocobalamin) (>96%, HPLC) were purchased from Fluka Chemical Corp. 3′-Dephospho-CoA, ethylenediaminetetraacetic acid, disodium salt (EDTA), 3-(*N*-morpholino)propanesulfonic acid (MOPS), 2-mercaptoethanesulfonic acid, sodium salt (coenzyme M), 1,4-dithio-DL-threitol (DTT), and bromelain (EC 3.4.22.32) from pineapple stem were obtained from Sigma Chemical Co. β-[3-^{14}C]Alanine (55 mCi/mmol) was purchased from American Radiolabeled Chemicals (St. Louis, MO). Ferredoxin was purified from acetate-grown cells of *Methanosarcina barkeri* as previously described (*7*). Unless otherwise stated, all other chemicals were commercial products of analytical grade.

[^{14}C]Coenzyme A. Coenzyme A specifically labeled with ^{14}C was obtained by purification from *Clostridium kluyveri* following growth in synthetic medium containing ^{14}C-labeled β-alanine. The medium was a modified version of that described by Bornstein and Barker (*8*). A 1 L culture of *C. kluyveri* was started with a 2% v/v inoculum and grown in the presence of 300 μCi of β-[3-^{14}C]alanine for 80 h (while maintaining the pH between 7.25 and 7.65 by periodic additions of K_2CO_3) to a final optical density at 600 nm of 0.62. The cells were harvested anaerobically by centrifugation at 3700*g* for 12 min, at 4 °C, and resuspended with 2 mL of cold anaerobic H_2O. Extraction was carried out by addition of 9 mL of anaerobic ethanol, 3 mL of 100 mM Tris-acetate (pH 8.5), and 150 μL of 1 M DTT, and the mixture was heated at 60 °C under a constant stream of N_2 for 60 min, cooled, and centrifuged at 11000*g* for 20 min. The supernatant fraction was adjusted to pH 4.5 with glacial acetic acid, and chromatographed on a QAE-cellulose column (2.5 cm × 12 cm) previously equilibrated with 50 mM potassium acetate and 5 mM DTT (pH 5.0). Most of the bound radioactivity was present in the CoASH peak, which eluted near the end of a 500 mL linear gradient of 0.05 to 1.0 M potassium acetate (pH 5.0) containing 5 mM DTT. The radioactive CoASH was further purified and desalted by adsorption on reversed phase Sep-Pak C_{18} cartridges and elution with methanol/water solutions, and the eluate was dried in vacuo. The specific radioactivity of the purified coenzyme A was 24.7 mCi/mmol. Anaerobic stock solutions were frozen and stored under liquid N_2.

ACDS Complex. The ACDS complex was isolated from acetate-grown *M. barkeri* by gel filtration on Sepharose CL-6B as described previously (*7*). Electrophoretic analysis indicated a purity of around 90% or greater, comparable to that shown previously (*7*). The preparation exhibited a specific activity of acetyl-CoA formation of ∼200 nmol min^{-1} (nmol of enzyme cobamide)$^{-1}$, as measured using bicarbonate as the carbonyl precursor and a Ti^{3+}−EDTA/ferredoxin reducing system similar to that previously described (*10*). Preparations of the enzyme complex were stored in liquid nitrogen. The protein was assayed by the method of Bradford (*9*), using bovine γ-globulin as a standard.

ACDS β-Subunit Preparation. Isolation of the β-subunit acetyltransferase component of the ACDS complex was carried out by a modification of the limited proteolytic digestion procedure described previously (*1*). The ACDS

complex (10.7 mg) was treated under anaerobic conditions with 350 μg of bromelain for 60 min at 24 °C in a reaction mixture (3.4 mL) that contained 1 mM L-cysteine-HCl and 50 mM MOPS buffer (pH 7.2). After incubation with bromelain, the reaction mixture was chromatographed on a Mono-Q HR 10/10 anion exchange column (Pharmacia Biotech) previously equilibrated with 50 mM Tris-SO_4 (pH 7.5). Elution was carried out at 2 mL/min with a linear gradient (250 mL) of 0 to 1 M Na_2SO_4 in 50 mM Tris-H_2SO_4 (pH 7.5). Fractions were collected at 2.5 min intervals. Three major protein peaks emerged from the column, the first of which contained the γ subunit and partially degraded forms of the δ subunit (δ*). The second protein component contained the α and ϵ subunits. The final peak contained a monomeric, truncated form of the β subunit (β*). Except as otherwise indicated, this purified fraction of the truncated β subunit was used in all kinetic experiments.

Super-Reducing Ti^{3+}−Citrate. Stock 140 mM Ti^{3+}−citrate reagent was prepared freshly before use by mixing in order 1 part by volume of 1.47 M $TiCl_3$ (Aldrich 19% w/w $TiCl_3$ in 20.4% w/w HCl) with 4.46 parts of 0.50 M trisodium citrate and then adding 5 parts of saturated Tris base; any other order of addition resulted in precipitation. The reagent was then diluted in 50 mM MOPS buffer (pH 7.2) to give a 10 mM Ti^{3+}−citrate working solution for direct addition to enzyme reaction mixtures. The $Ti^{4+/3+}$ midpoint reduction potential of the brown Ti^{3+}−citrate was estimated to be −0.75 V (NHE) or lower at pH 7.2 by titration of cob(II)alamin to co(I)alamin, monitored spectrophotometrically. In contrast, the purple-colored Ti^{3+}−EDTA complex, prepared as described previously (*10*), was incapable of converting cob(II)alamin to the Co^{1+} state. Titration with methylviologen yielded a value of −0.48 V (NHE) as the midpoint potential for the $Ti^{4+/3+}$−EDTA complex.

Acetyltransferase. The nonradioactive analysis of acetyltransferase activity (reaction 5) was carried out inside a Coy type anaerobic chamber with a modification of the protocol described previously (*1*). The redox potential was continuously measured throughout the progress of reactions and during assembly of the components by using a graphite indicator electrode with a Ag/AgCl reference electrode (calibrated against a saturated calomel electrode taken as −242 mV relative to the normal hydrogen electrode, NHE; all potentials are reported relative to the NHE). The standard reaction mixture (1.2 mL final volume) contained 100 μM acetyl-CoA, 200 μM 3′-dephospho-CoA, approximately 0.4 nmol of ferredoxin, a suitable amount of enzyme to be analyzed, 100 μM aquocobalamin, and 0.1 M MOPS buffer (pH 6.5) reduced with a predetermined amount of Ti^{3+}−citrate reagent to yield a final potential of −570 mV. Reducing agent was added to mixtures made up with all components except dephospho-CoA and the enzyme. Thereafter, the enzyme was added and the mixture allowed to equilibrate under stable redox potential conditions for 3−5 min. The reaction was initiated by addition of dephospho-CoA and allowed to proceed at 24 °C. Aliquots (60 μL) were withdrawn as a function of time and mixed with an equal volume of a solution containing 2 mM $TiCl_3$ and 500 mM sodium citrate (pH 4.0) to stop the reaction, and the mixtures were frozen in liquid N_2 for storage prior to HPLC analysis.

Analysis by reversed phase HPLC was carried out as described previously (*1*) with minor modifications which improved resolution and recovery, as follows. (1) Samples were thawed one at a time under nitrogen and immediately injected to prevent exposure to air. (2) Solvents were kept anaerobic by continuous sparging with helium. (3) The aqueous component used in gradient formation and for equilibration of the column was changed to 10 mM potassium phosphate (pH 6.5) containing 0.05 mM 2-mercaptoethanesulfonate. Reactant and product peak areas, obtained by integration of absorbance at 260 nm, were used for calculation of reaction rates. For each of the products formed and substrates consumed, peak area values fit well as a simple exponential function of time, and the initial rate of the reaction was determined on the basis of a fit of all four of the reaction components. Acetyl transfer at a rate of 1 μmol/min is defined as one unit (U) of activity.

Acetyl-CoA−CoA Isotope Exchange. Conditions used to monitor the exchange of [^{14}C]CoA into acetyl-CoA were identical to those described for analysis of acetyltransferase, with the exception that 3′-dephospho-CoA was absent and ^{14}C-labeled CoA was added to start the reaction. The total CoA concentration was varied in the range of 2−50 μM by initiating reactions with CoA solutions with different specific radioactivities, all of which contained the same total amount of radioactivity, 109 000 dpm/mL in the reaction. Analysis by HPLC was performed as described, except that fractions comprising the CoA and acetyl-CoA peaks were collected and analyzed for radioactivity by scintillation counting. In all cases, the ratio of radioactivity in the two peaks obtained at isotopic equilibrium agreed with that predicted on the basis of the amounts of acetyl-CoA and CoA added to the reaction mixture. The exchange reaction velocity (v*) was calculated as described by Segel (*11*) according to the following equation:

$$v^* = -\frac{[\text{CoA}][\text{acetyl-CoA}]}{[\text{CoA}] + [\text{acetyl-CoA}]}\frac{1}{t}\ln(1 - F)$$

in which F is the fraction of isotopic equilibrium attained at time t. Plots of $\ln(1 - F)$ versus t were linear to isotopic equilibrium, and the slopes were used to calculate the exchange velocity. One unit (U) is defined as a rate of 1 μmol/min. Kinetic parameters were determined as described by Fromm (*6*).

RESULTS

Acetyltransferase Redox Dependence. Acetyl transfer from acetyl-CoA to 3′-dephospho-CoA (reaction 5) was measured as described in Materials and Methods. In the absence of a suitable reducing agent, little or no acetyltransferase activity was observed, either by the intact complex or by the isolated β subunit protein, even under anaerobic conditions. High reaction rates were observed only when a strong reductant such as Ti^{3+}−EDTA or Ti^{3+}−citrate was used; milder reagents such as DTT were ineffective. Cobalamin was not required to support high levels of activity; however, addition of cobalamin afforded increased stability of redox potential measurements over a relatively wide range, and therefore, it was included in the standard reaction (Materials and Methods). The effect of varying the redox

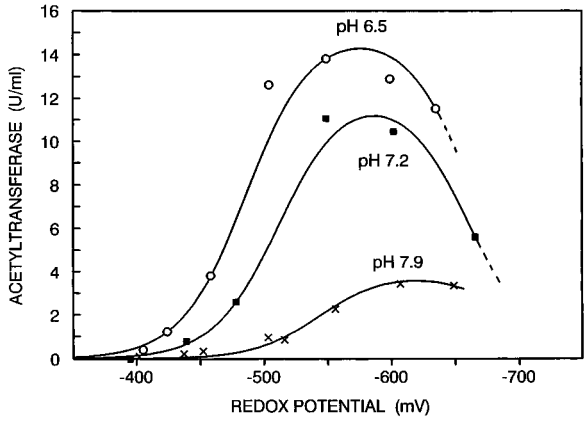

FIGURE 1: Redox dependence of acetyltransferase activity. The effect of redox potential on the rate of acetyl transfer (reaction 5) was examined at three different pH values: 6.5, 7.2, and 7.9. The redox potential was poised in the region of −400 to −700 mV (NHE) by addition of different amounts of Ti^{3+}−citrate to mixtures buffered at the indicated pH values under conditions otherwise equivalent to those of the standard reaction described in Materials and Methods. After potential stabilization, approximately 1 μg of the purified β subunit preparation was added and the mixture allowed to equilibrate for 3−5 min at that potential. Reactions were then initiated by the addition of 3′-dephospho-CoA to a final concentration of 200 μM (Materials and Methods). Aliquots removed from reaction mixtures as a function of time were subsequently analyzed by HPLC, and initial rates were calculated on the basis of the time-dependent changes in reactant and product concentrations, as described in Materials and Methods. The lines were drawn to represent a process involving two redox changes, one being an apparent one-electron activation of the enzyme and the other causing inactivation at potentials at least 100 mV more negative.

potential on the rate of acetyl transfer was examined at three different values of pH, as shown in Figure 1. Acetyltransferase activity was minimal at potentials higher than −400 mV, but increased markedly as the potential was decreased to more negative values. Half-maximal rates were achieved at redox potentials of −486, −512, and −544 mV at pH values of 6.5, 7.2, and 7.9, respectively. The shift in midpoint potential was approximately −40 mV/pH unit. This degree of influence by pH suggested that protons are involved in the reduction process to the extent of about 0.7 mol of H^+ per equivalent of electrons. The measurement of redox potentials around −700 mV and below was limited by the standard potential of the Co^{2+}/Co^{1+} couple of cobalamin acting as a mediator. However, at this limit, acetyltransferase activity was substantially diminished, and at lower potentials generated with excess amounts of Ti^{3+}−citrate, activity was lost entirely. Low reaction rates were also observed in control reactions both with excess Ti^{3+} in the absence of cobalamin and with cob(I)alamin in the absence of Ti^{3+} (generated in situ as a product of the reaction of methylcobalamin with 2-mercaptoethanesulfonate catalyzed by purified *M. barkeri* methylcobamide:2-mercaptoethanesulfonate methyltransferase). Thus, loss of activity appears to be related to the effect of very low redox potential in general, and is not specifically due to either the Ti^{3+} reagent by itself or the presence or absence of cob(I)alamin.

Kinetics of Acetyltransferase. To determine the kinetic mechanism of acetyltransferase, steady state kinetic experiments were performed in which the concentration of acetyl-CoA was varied at different fixed levels of 3′-dephospho-CoA. Two different conditions of pH and redox potential were investigated, one in which the enzyme was fully activated using Ti^{3+}−citrate to generate a potential of −570 mV at pH 6.5 and the other in which activation was incomplete in the presence of Ti^{3+}−EDTA, affording a substantially less negative potential at pH 7.2. Under incompletely reducing conditions, plots of the initial rate versus acetyl-CoA concentration were sigmoidal, indicating a cooperative dependence on acetyl-CoA concentration. Sigmoidal kinetics were found both with the intact ACDS complex and with the β subcomponent monomer, thus excluding the possibility that cooperativity was related to oligomeric interactions. Although parallel straight lines would be expected for a simple ping-pong mechanism, double-reciprocal plots of the data yielded curved lines with parallel tangents, as shown in Figure 2A. Nevertheless, the results still fit a ping-pong mechanism, only modified to include an additional step in which acetyl-CoA also binds to the oxidized form of the enzyme.

Under fully activating conditions (pH 6.5 and −570 mV), the sigmoidal pattern was eliminated, and hyperbolic kinetics were observed, as shown in Figure 2B. Double-reciprocal plots yielded a family of parallel straight lines, and the data were analyzed according to a simple ping-pong mechanism, as described by eq 7.

$$\frac{1}{v} = \frac{K_m^{\ A}}{V_{max}[A]} + \frac{K_m^{\ B}}{V_{max}[B]} + \frac{1}{V_{max}} \qquad (7)$$

The secondary plots shown in Figure 3 were used to obtain values of the true kinetic parameters for K_m for acetyl-CoA ($K_m^{\ A}$) of 30.8 μM and K_m for 3′-dephospho-CoA ($K_m^{\ B}$) of 42.2 μM. The V_{max} was determined (Figure 3A) to be 61.9 μmol min^{-1} mg^{-1}, corresponding to a k_{cat} of 3100 min^{-1}. The modified ping-pong mechanism shown in Figure 4 was consistent with all of the kinetic behavior observed both under fully active conditions and under conditions in which part of the enzyme exists in an inactive oxidized state.

CoA Product Inhibition Analysis. The rate of acetyl transfer to 3′-dephospho-CoA was markedly decreased in the presence of low concentrations of the product CoA. Therefore, a kinetic analysis of product inhibition was performed to obtain further insight into the interaction of the enzyme with CoA and acetyl-CoA. Initial rate measurements were made under fully activating conditions of pH and redox potential, as described in Materials and Methods. The acetyl-CoA concentration was varied at a fixed, nonsaturating level of 3′-dephospho-CoA in the presence of different levels of the inhibitor CoA. The results were analyzed according to eq 8, as described by Segel (*11*) for inhibition by product P in a ping-pong bi-bi system,

$$\frac{1}{v} = \frac{K_m^{\ A}}{V_{max}[A]}\left(1 + \frac{K_{ia}K_m^{\ B}[P]}{K_{ip}K_m^{\ A}[B]}\right) + \frac{1}{V_{max}}\left(1 + \frac{K_m^{\ B}}{[B]} + \frac{K_m^{\ B}[P]}{K_{ip}[B]}\right) \qquad (8)$$

and are shown plotted in Figure 5. The analysis yielded values for the K_i of CoA (K_{ip} = 6.8 μM) and for the K_i of acetyl-CoA (K_{ia} = 45.4 μM). The ratio of K_{ip}/K_{ia} was used

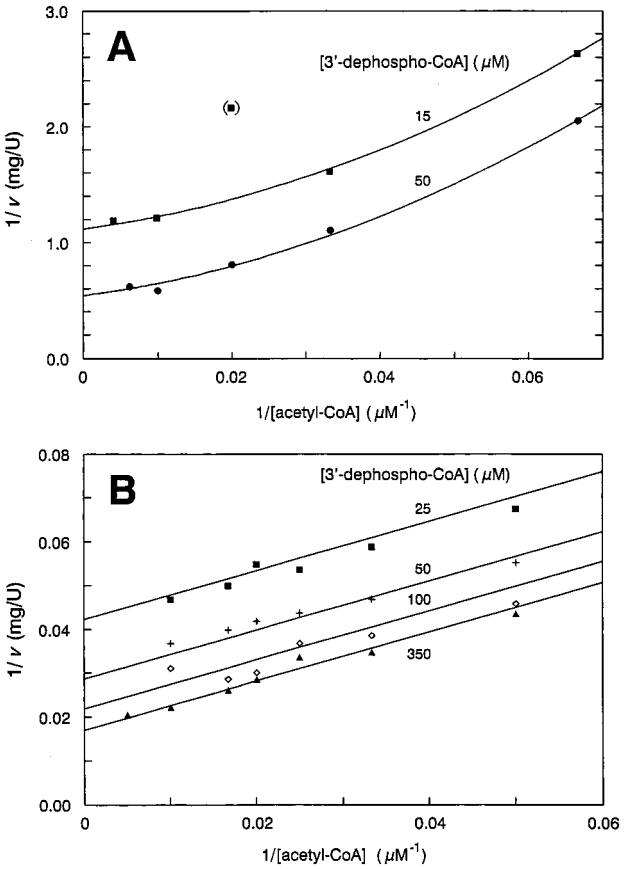

FIGURE 2: Acetyltransferase kinetics pattern under partially and fully activating reducing conditions. (A) The initial rate of acetyl transfer was measured under partially reducing conditions as a function of acetyl-CoA concentration at two different fixed levels of 3′-dephospho-CoA. Reaction mixtures contained 4.9 μg of the ACDS complex, and the reactions were set up in a manner similar to that of the standard reaction, as described in Materials and Methods. The acetyl-CoA concentration was varied from 20 to 240 μM in the presence of 15 or 50 μM 3′-dephospho-CoA. The reducing system contained ferredoxin in the presence of the milder reductant Ti^{3+}−citrate (4 mM) at pH 7.2 and lacked cobalamin. In test mixtures containing methylviologen as a mediator, the redox potential was measured at −540 mV in the absence of ACDS. However, the effective redox potential during the reactions was that set by ferredoxin in the presence of the enzyme complex, and is likely to be significantly less negative. Analysis of products and rate calculations were performed as described in Materials and Methods. The results are plotted according to the Lineweaver−Burke convention. (B) Acetyltransferase activity was measured under optimally reducing conditions as a function of acetyl-CoA concentration at different fixed levels of 3′-dephospho-CoA, using the stronger reducing system consisting of the brown Ti^{3+}−citrate complex and cobalamin (Co^{2+}/Co^{1+}) to establish a redox potential of −570 mV at pH 6.5. Reaction mixtures contained 0.53 μg of the β subunit protein and were assembled as indicated for the standard reaction mixture (Materials and Methods). Initial rates were calculated on the basis of the time-dependent change in reactant and product peak areas. The data were further analyzed according to eq 7, describing a ping-pong mechanism. The lines were drawn using the resulting values of the true kinetic parameters in the Lineweaver−Burke format.

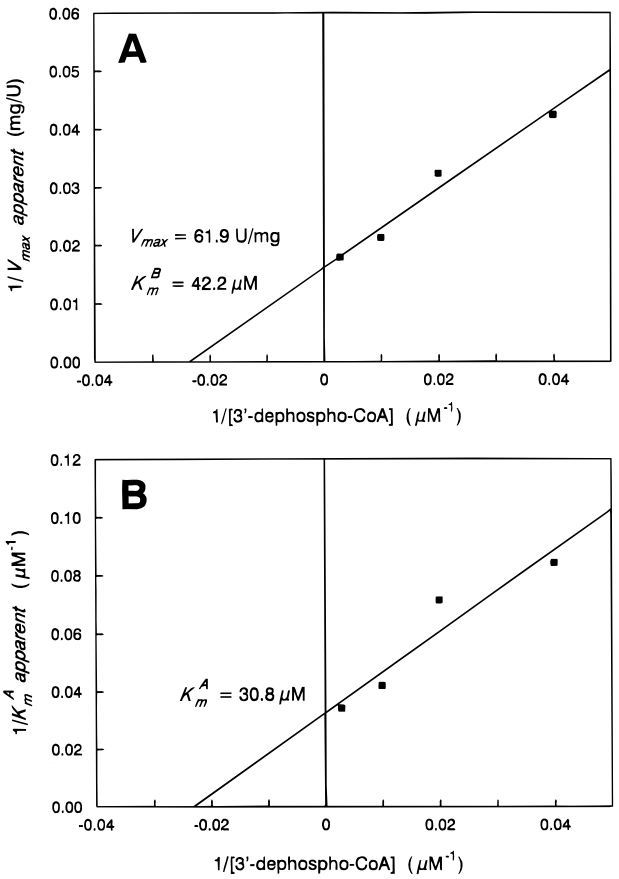

FIGURE 3: Secondary plot analysis of kinetic parameters. Kinetic data were analyzed to determine values of the true V_{max} and true K_ms for acetyl-CoA (K_m^A) and 3′-dephospho-CoA (K_m^B). The values of $1/V_{max}^{app}$ at each different level of 3′-dephospho-CoA were obtained by least-squares regression analyses carried out on each of the four data sets in Figure 2B. The $1/V_{max}^{app}$ values were then plotted vs 1/[3′-dephospho-CoA], as shown in panel A, which yielded the true V_{max} and K_m^B. The $1/K_m^{Aapp}$ values were also plotted against 1/[3′-dephospho-CoA], as shown in panel B, which provided the value for K_m^A.

to obtain the value for the equilibrium constant of eq 4 for acetyl-enzyme intermediate formation ($K_{eqF} = 0.15$). The free energy of hydrolysis of the acetyl-enzyme intermediate ($\Delta G^{\circ\prime}$ of eq 9) was thereby found to be −9.6 kcal/mol.[3]

$$E_\beta\text{-acetyl} + H_2O \rightleftharpoons E_\beta + \text{acetate} \qquad (9)$$

Kinetics of Acetyl-CoA/CoA Isotope Exchange. The kinetic pattern of the acetyl-CoA/CoA exchange reaction had not been previously established. Therefore, we carried out kinetic studies on the isotopic exchange reaction (reaction 6). In addition, this provided a method for characterizing interactions of the acetyl-enzyme intermediate independent of the substrate analogue 3′-dephospho-CoA. Reactions were set up as described in Materials and Methods, in which the concentration of CoA was varied at different fixed levels of acetyl-CoA. The exchange velocity was plotted versus CoA concentration in double-reciprocal form, as shown in Figure 6A. The results showed a pattern of parallel lines, indicating that the CoA exchange reaction also proceeds by a ping-pong kinetic mechanism. Kinetic parameters were obtained according to the method of Fromm (*6*) for analysis of the A ⇌ P portion of a ping-pong bi-bi system at chemical

[3] The $\Delta G^{\circ\prime}$ for hydrolysis of the acetyl-enzyme intermediate (E_β-acetyl) was obtained by subtracting the value of $\Delta G^{\circ\prime}$ found for reaction 4 from the known value of $\Delta G^{\circ\prime}$ for hydrolysis of acetyl-CoA (on the basis that the sum of reactions 4 and 9 yields the equation for the hydrolysis of acetyl-CoA). Reaction 4 was found to have a $\Delta G^{\circ\prime}$ of 1.1 kcal/mol on the basis of the value determined for the equilibrium constant K_{eqF}. The published value of −8.5 kcal/mol was used as the standard free energy of hydrolysis of acetyl-CoA (*13*).

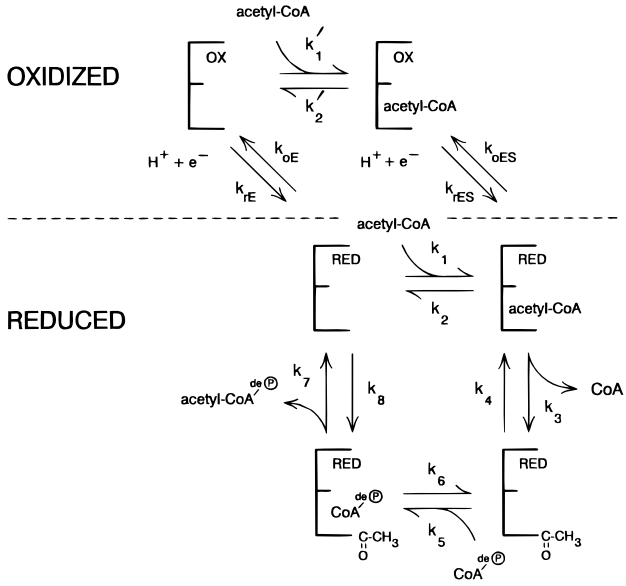

FIGURE 4: Kinetic mechanism for redox-dependent ACDS acetyltransferase. A modified ping-pong mechanism is shown consistent with the kinetic results obtained both under partially reducing conditions and under fully reduced and active conditions. Inactive OXIDIZED and active REDUCED forms of the enzyme capable of binding acetyl-CoA are depicted in redox equilibrium. Higher-order, cooperative dependence on acetyl-CoA concentration is predicted under conditions in which a significant portion of the enzyme exists in the oxidized form. When all of the enzyme is in the fully reduced active form, the reaction sequence simplifies to an elementary ping-pong mechanism, consisting of reactions in the lower REDUCED part only. Under these conditions, the definition of $k_{cat} = k_3k_7/(k_3 + k_7)$ applies, and $V_{max} = k_{cat}E_{total}$. The expressions for K_m^A (for acetyl-CoA) and K_m^B (for 3′-dephospho-CoA) are given as follows: $K_m^A = [k_7(k_2 + k_3)]/[k_1(k_3 + k_7)]$ and $K_m^B = [k_3(k_6 + k_7)]/[k_5(k_3 + k_7)]$. Steps involving k_1/k_2 and k_3/k_4 (which are constituents of reaction 4) denote the formation of the acetyl-enzyme intermediate from acetyl-CoA and the reduced fully active enzyme.

equilibrium (reaction 10),

$$F + P^* \underset{k_3}{\overset{k_4}{\rightleftharpoons}} [FP \leftrightarrow EA] \underset{k_1}{\overset{k_2}{\rightleftharpoons}} E + A \qquad (10)$$

in which P stands for the initially labeled species CoA, F denotes the acetyl-enzyme intermediate, EA and FP represent the central Michaelis complexes, E is the reduced active enzyme, A stands for acetyl-CoA, and the rate constants are as indicated in Figure 4. Reaction 10, which is the expanded form of reaction 4 in reverse, is described by the steady state rate expression given by eq 11.

$$\frac{1}{v^*} = \frac{k_2 + k_3}{k_2k_4E_{tot}}\left(\frac{1}{[P]} + \frac{K_{ia}}{K_{ip}[A]} + \frac{1}{K_{ip}}\right) \qquad (11)$$

The intercept term of eq 11, evaluated from plots of $1/v^*$ versus 1/[P] (Figure 6A), was plotted as a function of 1/[A], as shown in Figure 6B. The results yielded the value for K_{ia} of 120 μM and for K_{ip} of 32.2 μM. The value of the equilibrium constant of reaction 4 ($K_{eqF} = 0.27$) was obtained from the K_{ip}/K_{ia} ratio. From this, the free energy of hydrolysis of the acetyl-enzyme intermediate was calculated as −9.3 kcal/mol. The replot in Figure 6B yielded a value for V_{max}* of 54.2 μmol min^{-1} mg^{-1}, which corresponds to a k_{cat}* of 2710 min^{-1}.

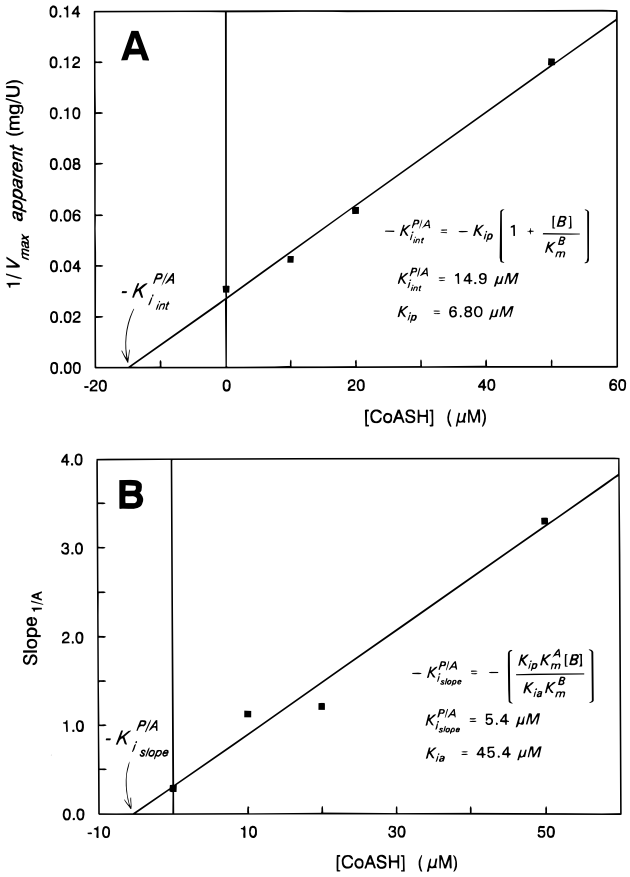

FIGURE 5: Acetyltransferase product inhibition kinetics. The extent of inhibition of acetyltransferase by the product CoA was measured in reactions in which acetyl-CoA concentration was varied in the presence of 50 μM 3′-dephospho-CoA under conditions of pH and redox potential yielding maximal activity. Reaction mixtures were set up as described in Materials and Methods except that 3′-dephospho-CoA and the inhibitor CoA were introduced together as a mixture to produce final concentrations of CoA in the range of 0−50 μM. Product analysis by HPLC and evaluation of initial rates were performed as indicated in Materials and Methods. Primary plots of the results were constructed in the double-reciprocal form (not shown), and these were further analyzed to obtain kinetic constants K_{ia} and K_{ip}, according to Segel (*11*). Values of $1/V_{max}^{app}$ from the primary plots are shown as a function of CoA concentration (A). The *X*-intercept of the plot in panel A gives $-K_i^{P/A}{}_{int}$, defined as indicated. The dissociation constant of the central complex involving CoA and the acetyl-enzyme intermediate ($K_{ip} = k_3/k_4$, Figure 4) was then obtained from the relationship $K_i^{P/A}{}_{int} = K_{ip}(1 + [B]/K_m^B)$, using the determined value for K_m^B of 42.2 μM, and [B] = 50 μM. In panel B, the slopes from the primary plots are shown as a function of CoA concentration, yielding $-K_i^{P/A}{}_{slope}$. The value of the dissociation constant of the complex involving acetyl-CoA and the reduced enzyme ($K_{ia} = k_2/k_1$, Figure 4) was determined from the value of $K_i^{P/A}{}_{slope}$, as indicated.

DISCUSSION

The overall synthesis or cleavage of the C−C bond of acetate (as acetyl-CoA) is brought about by the ACDS multienzyme complex in methanogens and at least one other genus of Archaea (*12*), and by a system of several enzymes in clostridia that are not found associated as a complex. Since many of the partial reaction steps leading up to the central reaction of making and/or breaking the acetyl C−C bond are not well characterized, it is therefore not surprising that the mechanism of the central reaction itself is still not established. By analogy to known inorganic reactions, it has

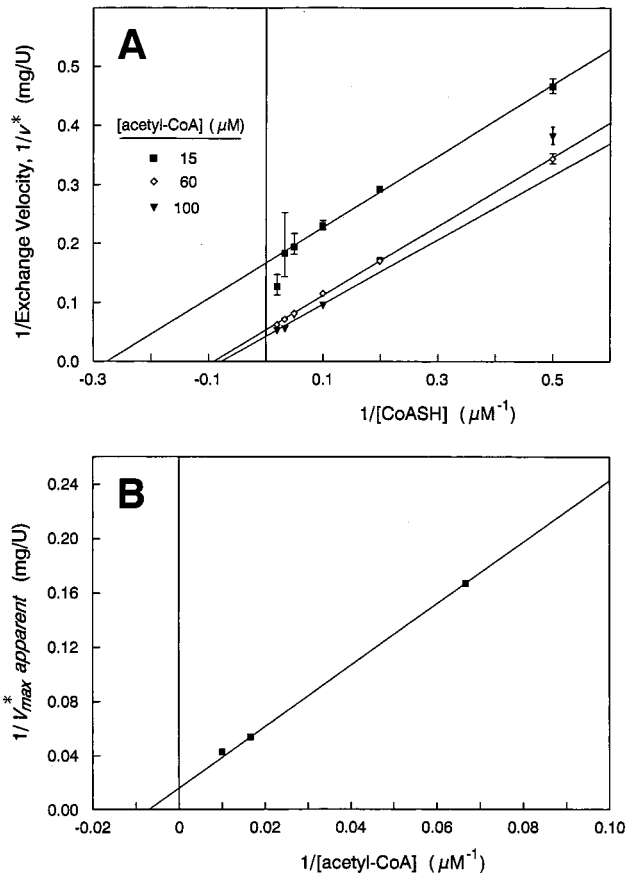

FIGURE 6: Kinetics of acetyl-CoA/CoA exchange. The CoA exchange reaction was performed as described in Materials and Methods. (A) Double-reciprocal plot of exchange velocity vs CoA concentration at different fixed levels of acetyl-CoA. (B) Replot of the *Y*-intercept (apparent $1/V_{max}$*) from the double-reciprocal plots vs reciprocal acetyl-CoA concentration. The *X*-intercept of this replot gave the value of K_{ia}. The replot in panel B also afforded values for K_{ip} and k_{cat}*, defined as $k_2k_3/(k_2 + k_3)$.

been suggested that enzymatic decarbonylation could involve metal-based insertion into the C−S and C−C bonds of acetyl-CoA. It is assumed that the first step in C−C fragmentation after binding of the substrate would be the transfer of the acetyl group from acetyl-CoA to the enzyme, to form an acetyl-metal species, involving possibly Fe or Ni. Studies by Ramer et al. (*3*), Lu and Ragsdale (*4*), Grahame et al. (*14*), and Barondeau and Lindahl (*15*) all suggest formation of an acetyl-enzyme intermediate. EPR studies are consistent with the possibility that this species is EPR-silent (*14*, *15*), making it difficult or impossible to characterize by that method. The acetyl-metal intermediate is proposed to undergo fragmentation to yield separately bound carbonyl and methyl species. The alternative fate would be transfer of the acetyl group back to an acceptor (e.g., CoA to form acetyl-CoA) or hydrolysis to produce acetate. The possibility that an acetyl-Ni species is involved has been raised in the studies of Barondeau and Lindahl (*15*), who demonstrated the importance of Ni for the functional methylation of clostridial acetyl-CoA synthase.

The existence of an acetyl-enzyme species was earlier suggested by the discovery of an acetyl-CoA/CoA exchange reaction catalyzed by both the ACDS multienzyme complex from *M. thermophila* and the CO dehydrogenase/acetyl-CoA synthase enzyme from *C. thermoaceticum* (*2*−*5*). The data presented here (Figures 2 and 6), however, show that this exchange reaction and the reaction of net acetyl transfer to 3′-dephospho-CoA both follow a ping-pong kinetic mechanism. This result does not support the alternative mechanism of CoA exchange by way of an [enzyme·CoA·acetyl-CoA] ternary complex. The finding of a ping-pong kinetic pattern therefore provides the strongest indication to date for the formation of an acetyl-enzyme species.

Redox Activation of Acetyl Transfer and Alteration of the Kinetic Pattern. The data shown in Figure 1 demonstrate that acetyl transfer activity depends on both pH and redox potential. The strong dependence on low redox potential is consistent with earlier results from the study by Lu and Ragsdale (*4*). Our data show, in addition, that inhibition occurs if the potential is too low. Furthermore, we show that changes in the redox potential result in alterations to the observed kinetic pattern. The rate of acetyl transfer exhibited a cooperative dependence on acetyl-CoA concentration under conditions in which reductive activation was incomplete, but showed hyperbolic kinetics under fully active reducing conditions. Changes in pH had a significant effect on the redox midpoint potential required for activation, indicating that a proton is taken up by the enzyme during reduction to the active form. The modified ping-pong mechanism shown in Figure 4 is a minimal kinetic model consistent with all of the observed effects of substrate concentration, pH, and redox potential. Under conditions in which all of the enzyme is in the fully reduced active state, the mechanism simplifies to that of an ordinary ping-pong mechanism, corresponding to the reactions only in the lower part of Figure 4.

Stability of the Acetyl-Enzyme Intermediate and the Relevance to the Mechanism of C−C Bond Formation and Cleavage. It has been known for many years that methanogenesis from acetic acid requires an activated form of acetate (*16*). Subsequently, it was shown that acetyl-CoA serves this function (*17*, *18*) and that binding of acetyl-CoA occurs on the β subunit of the methanogen acetyl-CoA decarbonylase/synthase complex (*1*). Our characterization of the thermodynamic stability of the resulting E_β-acetyl shows that it has a free energy of hydrolysis of around −9.3 to −9.6 kcal/mol. This indicates that a characteristic of the acetyl species undergoing C−C bond cleavage is that it is linked to the enzyme by a "high-energy" bonding interaction. Therefore, the need for an activated form of acetate can be understood since formation of the enzyme intermediate would require that the energy of the acetyl donor substrate be high enough to generate adequate levels of the activated acetyl-enzyme species. Acetyl-CoA satisfies this criterion for activation, and it is interesting to note that the energy of acetyl-enzyme interaction is even slightly higher than that of acetyl-CoA. Reductive activation is presumed to be involved with the formation of a nucleophilic center for attack on acetyl-CoA; however, the identity of the nucleophile (metal, or ligand to a redox-active metal?) and the nature of the bond between enzyme and acetyl are essential components of the mechanism that call for further investigation.

Kinetic Parameters and the Rate-Limiting Step in Acetyl Transfer. The kinetic parameters of K_{ia} (K_i for acetyl-CoA) and K_{ip} (K_i for CoA) were determined by two different kinds of steady state kinetic experiments. The first was based on analysis of CoA inhibition of the net reaction of acetyl

transfer to 3′-dephospho-CoA (reaction 5), and the second was based on analysis of the acetyl-CoA/CoA exchange reaction at chemical equilibrium (reaction 6). In principle, the K_i values derived from the two methods should be identical. However, it was found that the values were somewhat larger in experiments using isotope exchange analysis (which yielded a K_{ia} of 120 μM and a K_{ip} of 32 μM) than in studies on CoA inhibition (which gave a K_{ia} of 45 μM and a K_{ip} of 6.8 μM). Although this may suggest some fundamental difference between the two methods, nonetheless, relatively similar values were found for the K_{ip}/K_{ia} ratio. Thus, the equilibrium constant K_{eqF} for reaction 4 was established by the two methods to be between 0.15 and 0.27 (with the higher value given by the method of isotope exchange). The calculated values for the free energy of hydrolysis of the acetyl-enzyme intermediate were therefore also similar, with values of −9.6 kcal/mol obtained from the CoA inhibition data and −9.3 kcal/mol provided by isotope exchange analysis.

In the kinetic mechanism of acetyltransferase (Figure 4, lower portion), it is expected that if dissociation of acetyl-CoA is faster than formation of the acetyl-enzyme intermediate (i.e., $k_3 < k_2$), then the value of K_i for acetyl-CoA must always be equal to or greater than K_m^A. The value found for K_m^A of 30.8 μM is consistent with this condition. Furthermore, the finding that the value of K_{ia} does not greatly exceed that for K_m^A indicates that the step at which acetyl-enzyme formation occurs, k_3, contributes significantly to the overall k_{cat}. The observation of strong product inhibition by CoA also suggests that acetyl-enzyme formation may be largely rate-limiting. Furthermore, the finding that the value of k_{cat} (3100 min^{-1}) for reaction 5 is comparable to that of k_{cat}* (2710 min^{-1}) obtained from the isotope exchange reaction suggests that the rate of both reactions is limited at a common step. Thus, evidence indicates that enzyme-substrate binding and dissociation are fast relative to conversion to product ($k_3 < k_2$) and that the reaction rate is limited by the formation of the acetyl-enzyme intermediate (step k_3 in Figure 4).

Comparison of Kinetic Parameters with the Clostridial Enzyme. The "K_m" values for acetyl-CoA and CoA reported for the clostridial CO dehydrogenase/acetyl-CoA synthase (*3*, *4*) may be compared with caution to the corresponding K_i values that we obtained here. Although it was not mentioned in those papers, the parameters which were reported as K_m values for the acetyl-CoA/CoA exchange reaction in principle may be correctly interpreted as values of K_i. Caution is required because some uncertainty exists due to differences in experimental conditions (particularly redox potential, pH, and temperature), and because the kinetic mechanism had not been established in the previous studies. Nevertheless, if the previous K_m data are used, we calculate a value for the equilibrium constant for acetyl-enzyme formation K_{eqF} of approximately 0.03 (for the clostridial equivalent to eq 4). The value for the methanogen enzyme found here is 5−10 times larger than this, mainly as a result of a much smaller relative value of K_i for acetyl-CoA (45−120 μM) compared with the value of 1.5−1.9 mM for the clostridial enzyme. This implies that relative to that of CoA, the binding of acetyl-CoA may be tighter in the methanogen enzyme than in the case of clostridia, a possible benefit to methanogens in which acetyl-CoA serves as a substrate for cleavage. In addition, from the K_m data contained in the previous studies, we estimate the free energy of hydrolysis of the clostridial enzyme-acetyl intermediate to be −10.6 kcal/mol, or about 1 kcal/mol more negative than that of the methanogen enzyme. This indicates a possible advantage to formation of acetyl-CoA as a product in the acetogens by virtue of a relatively weaker binding to acetyl-CoA and more favorable thermodynamics for transfer of acetyl from the acetyl-enzyme intermediate to CoA.

It is more difficult to compare the K_d value for CoA binding to the clostridial enzyme reported earlier (*4*) to the K_i values for CoA that we determined here. This is because the K_i values reflect CoA binding to the F enzyme form (acetyl-enzyme intermediate), whereas the previous determination of K_d was made in the absence of strong reducing agents, and did not employ enzyme in the form of the acetyl-enzyme intermediate.

A comparison of the k_{cat}* values for CoA exchange must also be done with caution for reasons similar to those mentioned above. The value of 2710 min^{-1} (45 s^{-1}), which we determined at 24 °C, may be similar or perhaps greater than the value of 70 s^{-1} determined at 40 °C by Lu and Ragsdale (*4*) after taking into account the difference in temperature. Our value for k_{cat}* is substantially higher than the k_{obs} of 12 s^{-1} at 35 °C reported for the *M. thermophila* ACDS complex (*5*). This is most likely due to dissimilarities in assay conditions, since when we used 3′-dephospho-CoA as an acetyl acceptor, we did not find a large difference in acetyltransferase specific activity of ACDS prepared from *M. thermophila* versus *M. barkeri*.

ACKNOWLEDGMENT

We thank Dr. Wei-Ping Lu of Proctor & Gamble Pharmaceutical Health Care Research Center (Mason, OH) and Dr. Steve Ragsdale of The University of Nebraska (Lincoln, NE) for valuable insight from tests on reductive activation of the *M. barkeri* enzyme complex.

REFERENCES

1. Grahame, D. A., and DeMoll, E. (1996) *J. Biol. Chem. 271*, 8352−8358.
2. Pezacka, E., and Wood, H. G. (1986) *J. Biol. Chem. 261*, 1609−1615.
3. Ramer, S. E., Raybuck, S. A., Orme-Johnson, W. H., and Walsh, C. T. (1989) *Biochemistry 28*, 4675−4680.
4. Lu, W. P., and Ragsdale, S. W. (1991) *J. Biol. Chem. 266*, 3554−3564.
5. Raybuck, S. A., Ramer, S. E., Abbanat, D. R., Peters, J. W., Orme-Johnson, W. H., Ferry, J. G., and Walsh, C. T. (1991) *J. Bacteriol. 173*, 929−932.
6. Fromm, H. J. (1975) Isotope exchange, *Initial Rate Enzyme Kinetics*, Chapter VI, Springer-Verlag, New York.
7. Grahame, D. A. (1991) *J. Biol. Chem. 266*, 22227−22233.
8. Bornstein, B. T., and Barker, H. A. (1948) *J. Bacteriol. 55*, 223−230.
9. Bradford, M. M. (1976) *Anal. Biochem. 72*, 248−254.
10. Grahame, D. A., and DeMoll, E. (1995) *Biochemistry 34*, 4617−4624.
11. Segel, I. H. (1975) *Enzyme Kinetics*, John Wiley and Sons, New York.
12. Dai, Y.-R., Reed, D. W., Millstein, J. H., Hartzell, P. L., Grahame, D. A., and DeMoll, E. (1998) *Arch. Microbiol. 169*, 525−529.

13. Guynn, R. W., Golberg, H. J., and Veech, R. L. (1973) *J. Biol. Chem. 248*, 6957−6965.
14. Grahame, D. A., Khangulov, S., and DeMoll, E. (1996) *Biochemistry 35*, 593−600.
15. Barondeau, D. P., and Lindahl, P. A. (1997) *J. Am. Chem. Soc. 119*, 3959−3970.
16. Krzycki, J. A., Lehman, L. J., and Zeikus, J. G. (1985) *J. Bacteriol. 163*, 1000−1006.
17. Grahame, D. A., and Stadtman, T. C. (1987) *Biochem. Biophys. Res. Commun. 147*, 254−258.
18. Fischer, R., and Thauer, R. K. (1988) *FEBS Lett. 228*, 249−253.

BI9812423